1570 *J. Phys. Chem. A* **2005,** *109,* 1570−1575

Solvent-Dependent Vibrational Frequencies and Reorganization Energies of Two Merocyanine Chromophores

Weinan Leng,[†] Frank Würthner,[‡] and Anne Myers Kelley*[,†]

School of Natural Sciences, University of California, Merced, P.O. Box 2039, Merced, California 95344, and Institut für Organische Chemie, Universität Würzburg, Am Hubland, 97074 Würzburg, Germany

Received: October 25, 2004; In Final Form: December 22, 2004

Absorption and resonance Raman spectra have been measured over a wide range of solvents for two merocyanine dyes containing the indoline ("Fischer" base) electron donor group with different accepting groups. One appears to be near the cyanine limit (equal contributions of the neutral and zwitterionic resonance forms to both ground- and excited-state structures) based on electrooptic absorption data showing a very small dipole moment change upon electronic excitation. The resonance Raman spectra of both molecules show significant frequency shifts and intensity redistributions that evolve monotonically with increasing solvent polarity and are consistent with increasing zwitterionic character of the ground-state structure. The vibrational reorganization energies of both molecules, obtained by simulating the absorption band shapes, are smaller in polar solvents than in nonpolar or weakly polar ones, consistent with a more cyanine-like structure at higher solvent polarities. However, the vibrational reorganization energies of both molecules exceed 700 $\mathrm{cm^{-1}}$ in all solvents, larger than in many true cyanine dyes, and the optical absorption maxima do not correlate well with either solvent polarity or vibrational reorganization energy. This indicates some limitations to the structural conclusions that can be reached from the two-state model for π-conjugated donor−acceptor systems.

Introduction

Many organic molecules contain electron donor and electron acceptor groups connected through a π-conjugated bridge. The structures of such molecules can be written in two possible resonance forms, one neutral and the other zwitterionic, with formal charge transfer from donor to acceptor accompanied by interconversion between single and double bonds in the π-bridge (Figure 1). In the simplest picture of the electronic excitations of such molecules, the neutral and zwitterionic resonance structures are treated as basis states whose linear combinations compose the actual ground and lowest excited electronic states.[1−4] The relative contributions of the neutral and zwitterionic states to the true molecular eigenstates are functions of the donor and acceptor groups as well as the solvent and can be tuned by varying either or both. If the ground state is largely neutral and the excited state largely zwitterionic, electronic excitation produces a large change in both the charge distribution and the equilibrium bond lengths of the conjugated bonds. As the contribution of the zwitterionic form to the ground state increases, the ground state becomes more polar and the excited state less polar, and the difference in bond lengths between the two structures becomes smaller. In the limit where both resonance forms contribute equally to both electronic states, there is no change in dipole moment upon excitation and all of the conjugated bonds have equal bond orders of 1.5 in both ground and excited states. This is known as the cyanine limit by reference to the cyanine dyes, which, for symmetry reasons, have structures that are equal contributions of two resonance forms (Figure 2).

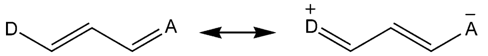

Figure 1. Neutral and zwitterionic forms of conjugated donor−acceptor substituted molecules.

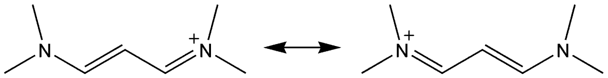

Figure 2. Equivalent resonance forms of a cyanine dye.

The ability to tune the ground-state charge-transfer character of these donor−acceptor substituted conjugated molecules is important because of its influence on the nonlinear optical properties. The two-state model for the ground and first excited electronic states[1,3] can be used to predict the dependence of the molecular polarizability and hyperpolarizabilities on the degree of ground-state charge transfer or, equivalently, the bond-order alternation in the ground state. The general predictions of this simple model are supported by semiempirical and ab initio molecular orbital and finite-field (hyper)polarizability computations.[5,6] The first hyperpolarizability (β) should be maximized at an intermediate degree of mixing given by $c^2 = 0.276$ or 0.724, where we define $\Psi_g = \sqrt{1-c^2}\psi_N + c\psi_Z$ and ψ_N and ψ_Z are the neutral and zwitterionic basis states, respectively. On the other hand, both the linear polarizability (α) and the second hyperpolarizability (γ) are maximized in the cyanine limit ($c^2 = 0.5$: equal contributions from both resonance structures, zero bond-order alternation). Interest in developing polar dyes that approach the cyanine limit has been driven by interest in these dyes as chromophores for photorefractive materials. Photorefractivity in organic chromophore-doped polymers with low glass transition temperatures is interpreted as a Kerr effect which has contributions from both the linear polarizability anisotropy and the first hyperpolarizability, but for typical chromophores the birefringent ($\delta\alpha$) contribution is dominant.[7,8] Optimization of chromophores for this purpose

---

[†] University of California.

[‡] Universität Würzburg.

10.1021/jp045145x CCC: $30.25

therefore corresponds to seeking the highest possible linear polarizability consistent with other requirements such as solubility, chemical compatibility, and thermal stability.[8,9]

The fractional charge-transfer character, or degree of bond-order alternation, in molecules of this type should be tunable by changing either the donor and/or acceptor strength or the polarity of the solvent. While many experiments have demonstrated such tuning of the ground-state structure and/or one or more optical properties,[10−19] rarely have both ground- and excited-state properties been examined for consistency with the predictions of the two-state model. Previous publications by the Kelley group utilized resonance Raman spectroscopy and intensity analysis to examine the solvent dependence of both the ground-state vibrational frequencies and the ground- to excited-state vibrational reorganization energies for several push−pull chromophores.[20−24] These were molecules far from the cyanine limit in which the ground state is predominantly neutral and has significant bond-order alternation. While the vibrational reorganization energy is found to decrease with increasing solvent polarity as expected by the simple two-state model, the ground-state structure as inferred from the vibrational frequencies is almost independent of solvent polarity, in contrast with the predictions of that model. It should be noted, however, that most of the molecules examined had largely aromatic rather than polyenic conjugated linkers, and the one largely polyenic molecule showed better consistency with the two-state model.[24] Other workers have also reported substantial solvent effects on ground-state vibrational spectra for push−pull molecules with mainly polyenic linkers.[13,18]

In this work we apply solvent-dependent resonance Raman and absorption spectroscopy to two merocyanine dyes of the class being developed as photorefractive chromophores (Figure 3). One of these dyes, *I*ndoline*D*imethinedi*O*xo*P*yridine (IDOP), appears to be near the cyanine limit in polar solvents, as its absorption spectrum exhibits a strong origin band with relatively weak vibronic structure. The other, *I*ndoline*D*imethine*M*alono*N*itrile (IDMN), couples the same donor group to a weaker acceptor and is farther from the cyanine limit as judged by its absorption band shape. Conversion between neutral and zwitterionic resonance structure does not require any loss of aromatic stabilization for these molecules, and therefore we might expect to observe larger solvent-dependent variations in ground-state bond order than in molecules containing aromatic linkers.

Experimental Methods

IDMN was synthesized according to ref 25, and IDOP was synthesized by the method described in ref 26. Both compounds were characterized by 200 MHz ^{1}H NMR spectroscopy in $CDCl_3$ (TMS as internal standard) and elemental analysis. IDOP: 8.03 ppm (2H, s, CH methine), 7.38 ppm (2H, m, CH aromat), 7.27 ppm (1H, m, CH aromat), 7.11 ppm (1H, d, $J = 7.9$ Hz, CH aromat), 4.06 ppm (2H, t, $J = 7.1$ Hz, NCH_2), 3.92 ppm (2H, m, NCH_2), 2.53 ppm (3H, s, CH_3), 1.9 ppm (3H, m, CH_2, CH), 1.73 ppm (6H, s, CH_3), 1.51 ppm (2H, m, CH_2), 1.31 ppm (8H, m, CH_2), 1.02 ppm (3H, t, $J = 7.4$ Hz, CH_3), 0.90 ppm (6H, m, CH_3). Anal. Calcd for $C_{31}H_{41}N_3O_2$: C, 76.35; H, 8.47; N, 8.62. Found: C, 76.37; H, 8.49; M, 8.61. mp: 158−160 °C.

Absorption spectra were measured on a Hitachi U-3010 UV/vis spectrophotometer.

Resonance Raman spectra were obtained at concentrations of 0.17−0.44 mM for IDMN and 0.088 mM for IDOP. Two different sampling and detection systems were employed. One was a 0.6-m Spex 1877E triple spectrograph utilizing reflective collection optics, a 1200 g/mm grating blazed at 500 nm in the spectrograph stage, and a liquid nitrogen-cooled CCD detector. Samples of ~3 mL volume were contained in a spinning cell, illuminated with 1−20 mW of laser power focused with a 10-cm f.l. lens, and the Raman scattering was collected in a ~135° backscattering geometry. The other was a 0.64-m Jobin-Yvon T64000 triple spectrograph with microprobe sampling (10× objective), either a 1200 g/mm grating blazed at 750 nm or an 1800 g/mm grating blazed at 500 nm in the spectrograph stage, and a UV-coated, back-illuminated, liquid nitrogen-cooled CCD detector. Samples of ~10-mL volume were circulated with a peristaltic pump through a 1-mm path-length liquid flow cell, excited with <5 mW of laser power, and Raman scattering was collected in a confocal 180° backscattering geometry. Excitation wavelengths between 458 and 514 nm were provided by either a Lexel argon-ion laser or a Coherent Innova 90C argon-ion laser. Wavelengths between 360 and 450 nm were obtained from a frequency-doubled Spectra-Physics Tsunami Ti:sapphire laser producing 1−2-ps pulses at 82 MHz. Excitation at 532 nm was provided by a Spectra-Physics Millennia frequency-doubled cw Nd laser. In both instruments the scattering was collected at 90° to the incident laser polarization direction and the scattered polarization was randomized by passage through a polarization scrambler placed before the spectrograph entrance slit. The intensities measured therefore correspond to the differential Raman cross section, $(d\sigma/d\Omega)_{\|+\perp}$. For the Raman polarization measurements, the laser polarization was purified by passage through a Glan−Taylor prism and a rotatable film polarizer was

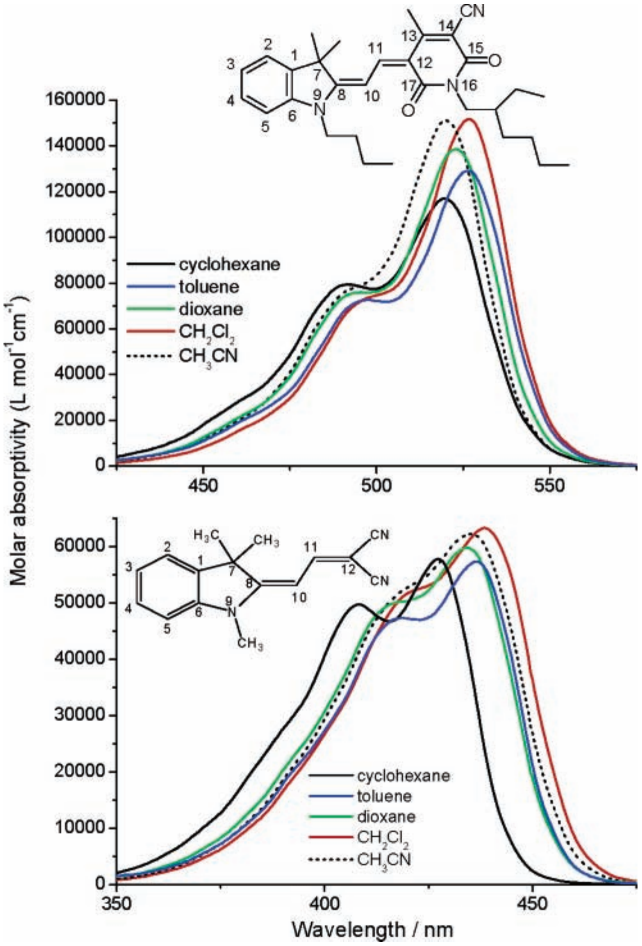

Figure 3. Absorption spectra of IDOP (top) and IDMN (bottom) in the indicated solvents. Atom numbering of the main carbon skeleton is shown.

placed in the scattered beam path before the polarization scrambler. Spectral resolution was 5−8 cm^{-1} for the argon-ion and Nd laser excited spectra and 11−14 cm^{-1} for the Ti:sapphire excited spectra. Spectra were calibrated in Raman shift by reference to Raman lines of the solvent. All spectra were obtained at ambient temperature (20−22 °C).

Computational Methods

Energy minimizations, normal mode calculations, and electronic structure calculations were carried out using the Gaussian 98 suite of programs[27] running under Windows. All alkyl groups were replaced by methyls. Ground-state normal mode calculations were performed using the B3LYP density functional with the 6-311G** and 6-31G** basis sets for IDMN and IDOP, respectively. The reported frequencies are unscaled. Qualitative normal mode descriptions were obtained by viewing the calculated normal mode motions with Molden 3.6.[28]

Absorption spectra were simulated via the time-domain wave packet method.[29] The vibronic structure was modeled as arising from four harmonic oscillators, each linearly coupled to the electronic excitation. Although the resonance Raman spectra show that there are many more than four coupled vibrations, inclusion of more modes does not significantly improve the calculated fits to the absorption spectra. Each mode was characterized by a vibrational frequency ω and a displacement Δ, in dimensionless normal coordinates, between the potential minima in the ground and excited states. The electronic line width was modeled as a Gaussian distribution of electronic zero−zero energies, which represents some combination of inhomogeneous broadening and coupling of the electronic transition to an overdamped Brownian oscillator representing the solvent degrees of freedom.[29,30] The vibrational displacements, electronic line width, and zero−zero energy were adjusted to obtain the best fit to the absorption band shape.

Results

Figure 3 shows the absorption spectra of IDOP and IDMN in five solvents of significantly different polarity and polarizability: cyclohexane, dioxane, toluene, dichloromethane, and acetonitrile. Spectra were also obtained in five other solvents. In both molecules the absorption maximum generally red-shifts with increasing solvent polarity and/or polarizability. The weak dependence of λ_{max} on solvent polarity for IDOP suggests that in this chromophore the change in charge distribution upon excitation is relatively small, again consistent with the idea that IDOP is fairly close to the cyanine limit. Both chromophores appear to exhibit a decrease in vibronic activity (i.e., the electronic zero−zero transition becomes relatively stronger compared with the higher vibronic transitions) as solvent polarity increases, although this is partially an illusion caused by the increase in absorption line width in the more polar solvents, making the vibronic structure appear less pronounced.

Figures 4 and 5 present the resonance Raman spectra of both chromophores in five solvents. Both molecules exhibit large solvent dependences in the intensities and/or frequencies of some modes. In IDMN, the two strong lines at 1540 and 1568 cm^{-1} in cyclohexane shift to considerably lower frequencies in more polar solvents while the line at 1134 cm^{-1} in cyclohexane moves to progressively higher frequencies with increasing solvent polarity. There are also large changes in the frequencies and/or intensities of the lines in the 1175−1250 cm^{-1} region, with the lines near 1176 and 1213 cm^{-1} gaining intensity in the more polar solvents while the 1234 cm^{-1} cyclohexane line is absent or strongly shifted in the other solvents. IDOP exhibits large solvent effects on both the frequencies and the intensities of the lines in the 1500−1700 cm^{-1} region. While the line at ~1540 cm^{-1} is strongest in all solvents and shifts only slightly in frequency, the lines at 1523, 1588, and 1690 cm^{-1} in cyclohexane all shift to lower frequencies with increasing solvent polarity (19−25 cm^{-1} from cyclohexane to acetonitrile) and undergo substantial intensity redistributions.

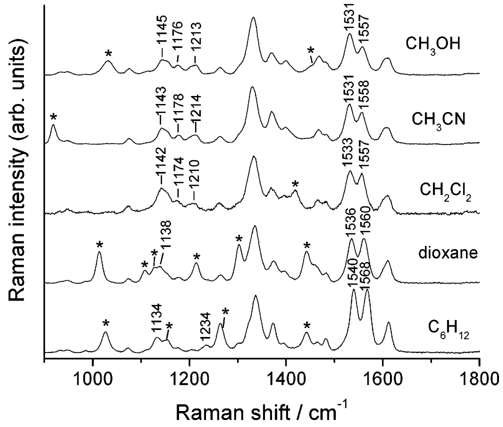

Figure 4. Resonance Raman spectra of IDMN in the five solvents indicated, all excited at 391 nm. Asterisks mark solvent lines. Frequencies that show large solvent dependences are labeled.

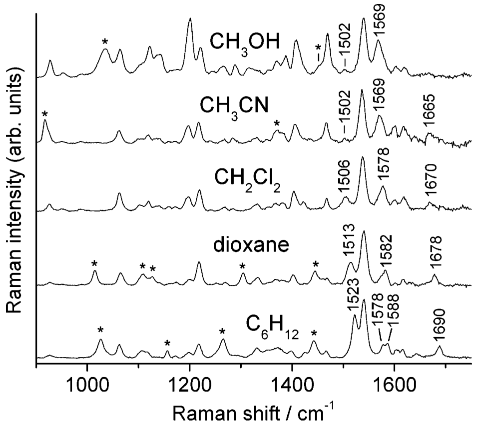

Figure 5. Resonance Raman spectra of IDOP in the indicated solvents. Excitation wavelength is 465 nm for methanol and 476 nm for the other four solvents. Asterisks mark solvent lines. Raman frequencies that show large solvent dependences are labeled.

The resonance Raman spectra in both Figures 4 and 5 were obtained using excitation wavelengths considerably to the blue of the absorption maximum. In the more polar solvents, fluorescence of both chromophores was sufficiently strong that adequate quality Raman spectra could not be obtained with excitation near the absorption maximum. Only in cyclohexane could complete excitation profiles be measured. In neither molecule do the vibrational frequencies in cyclohexane exhibit any significant dependence on excitation wavelength.

Tables 1 and 2 tentatively assign the prominent resonance Raman lines to the vibrational modes calculated with density functional theory. Figure 3 gives the atom numbering. In IDMN, the lines that exhibit the largest frequency reductions with increasing solvent polarity are assigned to modes having dominant contributions from the C_8C_{10} and $C_{11}C_{12}$ stretches. These are double bonds in the neutral structure but single bonds in the zwitterion, which should make a larger contribution to the structure in polar solvents. The lines in the 1125−1250 cm^{-1} region that undergo large changes in frequency and/or intensity with solvent are assigned to modes having large contributions from the $C_{10}C_{11}$, C_8N_9, or C_{12}−CN stretches, all of which are

TABLE 1: Experimental and Calculated (DFT, B3LYP/6-311G) Raman Frequencies for Prominent Lines of IDMN[a]**

IDMN Raman frequency/cm^{-1}						
cyclohexane	dioxane	CH_2Cl_2	methanol	CH_3CN	DFT calcd	DFT mode description
1073	1075	1075	1077	1074	1065	N−CH_3 str − C_1C_6 str − C_7C_8 str
1134	1138	1142	1145	1143	1180	asym. C−CN str
1176	1179	1173	1176	1176	1201	C_7C_8 str
1203	*	1206	1214	1214	1238	$C_{10}C_{11}$ str − C_8C_7 str + C_1C_7 str
1234	vw	1239	vw	vw	1273	$C_{10}C_{11}$ str − C_8C_7 str − C_1C_7 str
1263	1264	1262	1264	1264	1295	C_8N_9 str − C_1C_7 str
1337	1336	1332	1332	1330	1368	$C_{12}C_{15}$ str − $C_{11}C_{12}$ str, C_{11}H rock
1373	1374	1368	1370	1370	1384	C_3C_4 str + C_8N_9 str − C_4C_5 str − C_6N_9 str, C_{10}H rock
1395	1398	1396	1399	1398	1414	$(CH_3)_2$ rock, C_7C_8 str + N_9Me str
1465	1460	1465	1468	1467	1493	C_2C_3 str − C_5C_6 str
1482	1483	1481	1482	1483	1523	C_1C_6 str − C_6N_9 str
1540	1536	1533	1531	1531	1578	$C_{11}C_{12}$ str − C_8C_{10} str − $C_{10}C_{11}$ str
1568	1560	1557	1557	1568	1619	C_8C_{10} str − $C_{10}C_{11}$ str
1611	1610	1609	1610	1608	1657	C_5C_6 str + C_2C_3 str + C_8C_{10} str

[a] Asterisk indicates frequency regions obscured by solvent lines.

TABLE 2: Experimental and Calculated Resonance Raman Frequencies for IDOP[a]

IDOP Raman frequency/cm^{-1}						
cyclohexane	dioxane	CH_2Cl_2	methanol	CH_3CN	DFT calcd	mode description
1064	1065	1063	1064	1063	1068	N_9-alkyl str + C_{13}Me str
1108	*	1102	1106	1100	1100	acceptor ring def
1120	*	1120	1121	1118	1107	C_1C_7 str + donor ring def
1200	1202	1199	1200	1197	1244	$C_{12}C_{13}$ str + $C_{14}C_{15}$ str
1219	*	1219	1220	1216	1254	$C_{10}C_{11}$ str + C_1C_7 str
1332	1333	1333	1333	1330	1346	highly delocalized str
1399	1401	1409	1406	1406	1417	C_6N_9 str − N_9-alkyl str
1467	1468	1467	1469	1466	1502	C_2C_3 str − C_5C_6 str
1523	1513	1506	1502	1502	1576	C_8C_{10} str + $C_{13}C_{14}$ str − C_8N_9 str − C_7C_8 str
1542	1541	1538	1538	1536	1593	$C_{11}C_{12}$ str + $C_{13}C_{14}$ str − $C_{10}C_{11}$ str
1588	1582	1578	1568	1569	1634	C_8C_{10} str + $C_{13}C_{14}$ str − $C_{10}C_{11}$ str
1606	1602	1599	1603	1599	1655	C_1C_6 str + C_3C_4 str − C_4C_5 str − C_1C_2 str
1618	1618	1619	1619	1616	1667	C_5C_6 str + C_2C_3 str
1690	1678	1670	1670	1665	1762	sym C=O str

[a] Asterisks indicate frequency regions obscured by solvent lines.

formally single bonds in the neutral molecule and double bonds in the zwitterion. In IDOP, the highest-frequency (except for CH stretches) mode that exhibits the strongest solvent sensitivity is clearly assigned as predominantly C=O stretching, while the significantly solvent-dependent lines at 1588 and 1523 cm^{-1} (in cyclohexane) both have large contributions from the C_8C_{10} stretch.

In previous work on conjugated push−pull chromophores, the absorption spectra and resonance Raman intensities were modeled self-consistently to obtain the solvent and vibrational reorganization energies as a function of solvent.[20−22,24] Raman excitation profile analysis was needed to extract vibrational reorganization energies because the absorption spectra in the more polar solvents were too diffuse to allow the relative contributions of solvent and vibrational reorganization to be deduced. In the two molecules studied here, we could obtain complete excitation profiles only in cyclohexane because of the stronger fluorescence in more polar solvents. However, because the absorption spectra retain some vibrational structure even in polar solvents, it is possible to make a reasonable estimate of the vibrational reorganization energy by fitting the absorption spectra alone. The absorption spectra of both molecules in 10 different solvents were modeled by assuming four vibrations with frequencies of 600, 1000, 1350, and 1550 cm^{-1}, chosen to span the observed modes with significant Franck−Condon activity (both molecules have several Raman lines of moderate intensity in the 400−850 cm^{-1} range, but this region of the spectrum shows only weak solvent dependence and is not plotted in Figures 4 and 5). The displacement parameters of all four modes were adjusted, along with the electronic zero−zero energy and the line width, to best fit the absorption spectra. The line width was assumed Gaussian with a full width at half-maximum of 805 cm^{-1} for IDOP and 925−1175 cm^{-1}, depending on solvent, for IDMN. The reorganization energy arising from the high-frequency molecular vibrations was then obtained as

$$\lambda_{\mathrm{vib}} = \sum_{i=1}^{4} \frac{1}{2}\Delta_i^2\omega_i$$

Table 3 gives the results for both chromophores, and Figure 6 shows an example of a four-mode fit to the absorption spectrum of IDMN in tetrahydrofuran.

The vibrational reorganization energies of both molecules are significantly larger in cyclohexane, toluene, and dioxane than in the more dipolar solvents. Among the more dipolar solvents, variations in λ_{vib} are fairly small and are probably not significant (the estimated uncertainties in the best-fit values of λ_{vib} are about ±5%). When all 10 solvents are included, neither the absorption maximum nor the first moment of the absorption spectrum (a better measure of vertical excitation energy) correlates very well with solvent dipolarity or polarizability (refractive index) or any of their combinations often used to describe polar and nonpolar solvation.[31] However, all of the solvent shifts are quite small (a maximum of 8.5 nm for IDOP and 12.5 nm for IDMN). If the comparison is limited to the seven more polar solvents, the absorption spectrum of IDOP is seen to shift smoothly to lower

TABLE 3: Absorption Maximum (λ_{max}), First Moment of Absorption Spectrum ($\bar{\nu}_{mean}$), and Vibrational Reorganization Energy (λ_{vib}) for the Two Chromophores in Ten Solvents, along with the Refractive Index (n_D) and Dielectric Constant (ϵ) for Each Solvent at 20 °C

solvent	n_D	ϵ	IDOP λ_{max} (nm)	IDOP $\bar{\nu}_{mean}$ (cm^{-1})	IDOP λ_{vib} (cm^{-1})	IDMN λ_{max} (nm)	IDMN $\bar{\nu}_{mean}$ (cm^{-1})	IDMN λ_{vib} (cm^{-1})
cyclohexane	1.426	2.023	519.5	19988	1000	427.5	24390	1220
1,4-dioxane	1.422	2.029	523	19767	860	434	23878	1180
toluene	1.496	2.379	526.5	19708	880	436.5	23770	1180
chloroform	1.446	4.806	528	19581	730	440	23552	1130
tetrahydrofuran	1.405	7.52	524.5	19704	770	435.5	23798	1150
dichloromethane	1.424	9.08	526.5	19612	710	438.5	23602	1090
acetone	1.359	20.7	521.5	19751	740	435.5	23759	1110
ethanol	1.361	24.3	523	19736	770	436	23708	1170
methanol	1.329	33.62	519.5	19833	800	435.5	23714	1120
acetonitrile	1.344	36.6	520	19782	740	435	23736	1100

energies as solvent refractive index (polarizability) is increased. The same general trend is observed for IDMN, but it is less clear (Figure 7). It should be noted that protic solvents (ethanol and methanol) often behave anomalously because of hydrogen bonding interactions and also that toluene and dioxane, which have large quadrupole moments, tend to behave as solvents of somewhat higher dielectric constant in solvatochromic experiments.

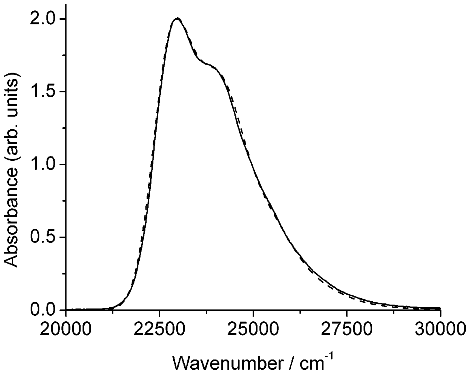

Figure 6. Experimental absorption spectrum of IDMN in tetrahydrofuran (solid) and spectrum calculated from 4-mode model (dashed).

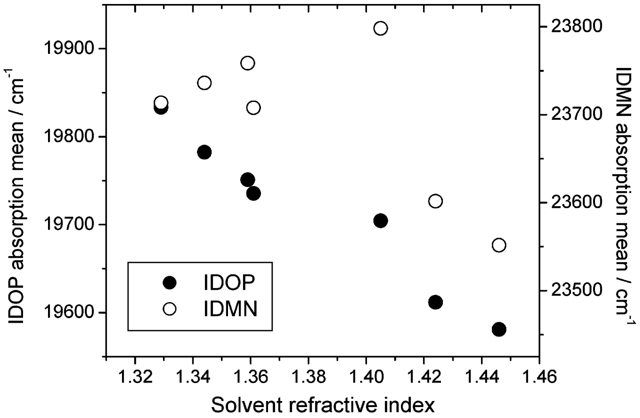

Figure 7. First moments of the absorption spectra for IDOP and IDMN plotted as functions of solvent refractive index. Only the seven most polar solvents of Table 3 are included.

Discussion

The commonly employed two-state valence-bond model for the structure of "push−pull" conjugated molecules treats the neutral and zwitterionic resonance structures of Figure 1 as basis states whose linear combinations compose the actual ground and first excited electronic states. An increased contribution from the zwitterionic form to the ground-state structure must therefore be accompanied by a decrease of equal magnitude in the contribution of the zwitterion to the excited-state structure. It is expected that in both IDOP and IDMN the neutral basis state will be lowest in energy in nonpolar solvents. As the solvent polarity and/or polarizability are increased, we expect the electronic transition to red-shift as the energy gap between neutral and zwitterionic basis states is reduced, while the vibrational reorganization energy should decrease as the neutral and zwitterionic basis states make more nearly equal contributions to both electronic eigenstates. If the point is reached at which the neutral and zwitterion have equal energies, the vibrational reorganization energy should go to zero and the electronic excitation energy should reach a minimum. Further increases in solvent polarity/polarizability should then start to reverse these changes, blue-shifting the absorption maximum and again increasing the vibrational reorganization. In contrast, because increasing solvent polarity always increases the contribution of the zwitterionic form to the ground-state structure, the ground-state vibrational frequencies and normal mode descriptions should change monotonically with increasing solvent polarity even if the cyanine limit is reached and/or passed.

Our observations are reasonably consistent with the conclusion that IDOP is quite close to the cyanine limit, at least in polar solvents. The absorption maximum in polar solvents is a function of solvent polarizability rather than solvent polarity, as expected for a conjugated structure having zero or small change in dipole moment upon excitation.[31] This conclusion is supported by the small (<2 D) ground- to excited-state dipole moment change obtained through electrooptic absorption measurements in dioxane on a very closely related structure that differs only in the alkyl groups.[9] However, the reorganization energy in all solvents examined is significantly greater than zero, indicating that the structural implications of the two-state model in the cyanine limit should not be taken too literally; that is, there are still nonnegligible changes in some of the bond lengths and/or angles upon electronic excitation. The resonance Raman spectra are not fully interpretable without definitive normal mode assignments, but they do change in a monotonic manner as solvent polarity is increased. The spectra of Figure 5 show a clear qualitative evolution from a nonpolar solvent (cyclohexane) to highly polar solvents (acetonitrile and methanol), with the spectra in CH_2Cl_2 appearing intermediate between them. IDMN also exhibits the expected monotonic evolution of its vibrational spectrum with solvent polarity. Both the more extended vibronic structure in IDMN's absorption spectrum and the more complicated solvent dependence of its absorption maximum would imply that it is farther from the cyanine limit than IDOP. This conclusion is supported by dipole moment data derived from electrooptical absorption spectroscopy, which found the dipole moments of IDMN in dioxane to be 9.0 D in the ground state and 12.7 D in the excited state.[32] Thus the change in dipole moment upon excitation is significantly greater for IDMN than for IDOP. However, while the standard picture would imply that this molecule should become closer to the cyanine limit as solvent polarity is increased, the vibrational reorganization energies are not reduced much in the most polar solvents.

Comparison of these results to those for nominally symmetric, true cyanine dyes is hindered by the lack of data on solvent dependences of either vibrational reorganization energies or ground-state Raman spectra. The cyanine dyes are known for their tendency to form extended aggregates having significantly different optical properties from the monomers, and the aggregates have been the focus of most studies. Symmetric cyanines in their monomeric forms typically exhibit weakly structured absorption spectra in which the electronic origin band has the greatest intensity. While 1,1′-diethyl-2,2′-cyanine (pseudoisocyanine, PIC)[33] exhibits a ratio of origin to vibronic intensities intermediate between IDOP and IDMN, longer-chain cyanines such as HDITCP and IR125 in methanol[31] and PD2501 and PD1659 in methylene chloride,[34] as well as several shorter-chain thiacarbocyanines,[35,36] show reduced vibronic structure, weaker than for IDOP in any solvent. Thus, it appears that many symmetric cyanines, as well as a few merocyanines such as the ATOP dyes **3g** of ref 9 and **3** of ref 37, have smaller vibrational reorganization energies than do either IDOP or IDMN. The absorption maxima of HDITCP,[31] IR125,[31] and PIC[33] are all well correlated with solvent polarizability, not polarity, although these correlations are limited for solubility reasons to moderately polar solvents. These results are consistent with the notion that true cyanine dyes are well described as nearly equal contributions from the two resonance forms in Figure 2. Even in these symmetric molecules, however, electronic excitation induces nonzero changes in bond lengths and/or angles, as evidenced by the nonvanishing vibronic structure in the electronic spectra.

Acknowledgment. This work was supported by NSF Grants No. CHE-0109920 to Kansas State University and No. CHE-0342816 to the University of California, Merced. We thank Rüdiger Wortmann for communicating his unpublished electrooptic absorption data.

References and Notes

(1) Lu, D.; Chen, G.; Perry, J. W.; Goddard, W. A., III. *J. Am. Chem. Soc.* **1994**, *116*, 10679.

(2) Thompson, W. H.; Blanchard-Desce, M.; Hynes, J. T. *J. Phys. Chem. A* **1998**, *102*, 7712.

(3) Blanchard-Desce, M.; Barzoukas, M. *J. Opt. Soc. Am. B* **1998**, *15*, 302.

(4) Beckmann, S.; Etzbach, K.-H.; Krämer, P.; Lukaszuk, K.; Matschiner, R.; Schmidt, A. J.; Schuhmacher, P.; Sens, R.; Seybold, G.; Wortmann, R.; Würthner, F. *Adv. Mater.* **1999**, *11*, 536.

(5) Gorman, C. B.; Marder, S. R. *Chem. Mater.* **1995**, *7*, 215.

(6) Abbotto, A.; Beverina, L.; Bradamante, S.; Facchetti, A.; Klein, C.; Pagani, G. A.; Redi-Abshiro, M.; Wortmann, R. *Chem.−Eur. J.* **2003**, *9*, 1991.

(7) Wortmann, R.; Poga, C.; Twieg, R. J.; Geletneky, C.; Moylan, C. R.; Lundquist, P. M.; DeVoe, R. G.; Cotts, P. M.; Horn, H.; Rice, J. E.; Burland, D. M. *J. Chem. Phys.* **1996**, *105*, 10637.

(8) Würthner, F.; Wortmann, R.; Meerholz, K. *ChemPhysChem* **2002**, *3*, 17.

(9) Würthner, F.; Wortmann, R.; Matschiner, R.; Lukaszuk, K.; Meerholz, K.; DeNardin, Y.; Bittner, R.; Bräuchle, C.; Sens, R. *Angew. Chem., Int. Ed. Engl.* **1997**, *36*, 2765.

(10) Marder, S. R.; Beratan, D. N.; Cheng, L.-T. *Science* **1991**, *252*, 103.

(11) Marder, S. R.; Perry, J. W.; Bourhill, G.; Gorman, C. B.; Tiemann, B. G.; Mansour, K. *Science* **1993**, *261*, 186.

(12) Marder, S. R.; Gorman, C. B.; Tiemann, B. G.; Cheng, L.-T. *J. Am. Chem. Soc.* **1993**, *115*, 3006.

(13) Marder, S. R.; Perry, J. W.; Tiemann, B. G.; Gorman, C. B.; Gilmour, S.; Biddle, S. L.; Bourhill, G. *J. Am. Chem. Soc.* **1993**, *115*, 2524.

(14) Marder, S. R.; Cheng, L.-T.; Tiemann, B. G.; Friedli, A. C.; Blanchard-Desce, M.; Perry, J. W.; Skindhøj, J. *Science* **1994**, *263*, 511.

(15) Blanchard-Desce, M.; Alain, V.; Bedworth, P. V.; Marder, S. R.; Fort, A.; Runser, C.; Barzoukas, M.; Lebus, S.; Wortmann, R. *Chem.−Eur. J.* **1997**, *3*, 1091.

(16) Barzoukas, M.; Muller, J.; Fort, A.; Marder, S. R.; Alain, V.; Blanchard-Desce, M. *Proc. SPIE-Int. Soc. Opt. Eng.* **1996**, *2852*, 132.

(17) Alain, V.; Rédoglia, S.; Blanchard-Desce, M.; Lebus, S.; Lukaszuk, K.; Wortmann, R.; Gubler, U.; Bosshard, C.; Günter, P. *Chem. Phys.* **1999**, *245*, 51.

(18) Del Zoppo, M.; Castiglioni, C.; Gerola, V.; Zuliani, P.; Zerbi, G. *J. Opt. Soc. Am. B* **1998**, *15*, 308.

(19) Zuliani, P.; Del Zoppo, M.; Castiglioni, C.; Zerbi, G.; Marder, S. R.; Perry, J. W. *J. Chem. Phys.* **1995**, *103*, 9935.

(20) Moran, A. M.; Delbecque, C.; Kelley, A. M. *J. Phys. Chem. A* **2001**, *105*, 10208.

(21) Moran, A. M.; Kelley, A. M. *J. Chem. Phys.* **2001**, *115*, 912.

(22) Moran, A. M.; Egolf, D. S.; Blanchard-Desce, M.; Kelley, A. M. *J. Chem. Phys.* **2002**, *116*, 2542.

(23) Moran, A. M.; Bartholomew, G. P.; Bazan, G. C.; Kelley, A. M. *J. Phys. Chem. A* **2002**, *106*, 4928.

(24) Moran, A. M.; Blanchard-Desce, M.; Kelley, A. M. *Chem. Phys. Lett.* **2002**, *358*, 320.

(25) Coenen, M.; Pestemer, M. *Z. Elektrochem.* **1953**, *57*, 785.

(26) Würthner, F. *Synthesis* **1999**, 2103.

(27) Frisch, M. J.; Trucks, G. W.; Schlegel, H. B.; Scuseria, G. E.; Robb, M. A.; Cheeseman, J. R.; Zakrzewski, V. G.; Montgomery, J. A., Jr.; Stratmann, R. E.; Burant, J. C.; Dapprich, S.; Millam, J. M.; Daniels, A. D.; Kudin, K. N.; Strain, M. C.; Farkas, O.; Tomasi, J.; Barone, V.; Cossi, M.; Cammi, R.; Mennucci, B.; Pomelli, C.; Adamo, C.; Clifford, S.; Ochterski, J.; Petersson, G. A.; Ayala, P. Y.; Cui, Q.; Morokuma, K.; Malick, D. K.; Rabuck, A. D.; Raghavachari, K.; Foresman, J. B.; Cioslowski, J.; Ortiz, J. V.; Stefanov, B. B.; Liu, G.; Liashenko, A.; Piskorz, P.; Komaromi, I.; Gomperts, R.; Martin, R. L.; Fox, D. J.; Keith, T.; Al-Laham, M. A.; Peng, C. Y.; Nanayakkara, A.; Gonzalez, C.; Challacombe, M.; Gill, P. M. W.; Johnson, B. G.; Chen, W.; Wong, M. W.; Andres, J. L.; Head-Gordon, M.; Replogle, E. S.; Pople, J. A. *Gaussian 98*, revision A.7; Gaussian, Inc.: Pittsburgh, PA, 1998.

(28) Schaftenaar, G. *Molden 3.6*; CMBI: The Netherlands, 2000.

(29) Myers, A. B. In *Laser Techniques in Chemistry*; Myers, A. B., Rizzo, T. R., Eds.; Wiley: New York, 1995; p 325.

(30) Li, B.; Johnson, A. E.; Mukamel, S.; Myers, A. B. *J. Am. Chem. Soc.* **1994**, *116*, 11039.

(31) Yu, A.; Tolbert, C. A.; Farrow, D. A.; Jonas, D. M. *J. Phys. Chem. A* **2002**, *106*, 9407.

(32) Wortmann, R. Univ. Kaiserslautern, Kaiserslautern, Germany. Personal communication, 2004.

(33) Renge, I.; Wild, U. P. *J. Phys. Chem. A* **1997**, *101*, 7977.

(34) Lepkowicz, R. S.; Przhonska, O. V.; Hales, J. M.; Fu, J.; Hagan, D. J.; Van Stryland, E. W.; Bondar, M. V.; Slominsky, Y. L.; Kachkovski, A. D. *Chem. Phys.* **2004**, *305*, 259.

(35) Khimenko, V.; Chibisov, A. K.; Gorner, H. *J. Phys. Chem. A* **1997**, *101*, 7304.

(36) Noukakis, D.; Van der Auweraer, M.; Toppet, S.; De Schryver, F. C. *J. Phys. Chem.* **1995**, *99*, 11860.

(37) Würthner, F.; Thalacker, C.; Matschiner, R.; Lukaszuk, K.; Wortmann, R. *Chem. Commun.* **1998**, 1739.